All-Optical Logic Gates Based on Nonlinear Slot Waveguide Couplers

Takeshi Fujisawa and Masanori Koshiba

Division of Media and Network Technologies, Hokkaido University, Sapporo 060-0814, Japan

A novel design of all-optical logic gates based on nonlinear slot waveguide couplers is proposed. NOT, OR, and AND logic gates can be realized by simple single optical directional coupler configuration. Strong polarization dependencies of slot waveguides are effectively utilized for realizing polarization-independent optical directional couplers in linear regime and polarization-dependent all-optical switches in nonlinear regime. All the simulations performed in this paper are done for three-dimensional nonlinear channel waveguide structures by using rigorous numerical schemes based on full-vector finite-element method specially formulated for nonlinear optical waveguides.

OCIS codes: 130.3750, 190.3270, 190.4390, 230.1150, 230.3990, 230.5440

1. Introduction

Nonlinear optical devices have attracted considerable attention because of their applicability for future high-speed all-optical signal processing devices.[1] A nonlinear optical directional coupler is one of the most representative nonlinear optical devices and can be used for various all-optical signal processing operations.[2] Extensive theoretical[2-4] and experimental[5] researches have been done in this field so far. One of the possible applications of these nonlinear optical

devices is a logic gate. All-optical logic gates using optical Kerr effect as a switching mechanism have also been intensively studied theoretically. [6-12] These nonlinear logic gates are promising candidates for performing all-optically arithmetic operations. Some of the proposed logic gates utilize a weak nonlinearity in the waveguide[6,9,11] and these devices can be easily cascaded. However, because of weak nonlinearity, the device size is relatively large, and the structure becomes complex. On the other hand, logic gates using strong nonlinearity have also been proposed.[7,8,10,12] These devices utilize a spatial soliton to manipulate light. Although the device size is small, usually, it is difficult to cascade. Furthermore, almost all the simulations were done in two-dimensional nonlinear slab waveguide geometries.[7,10-12]

In this paper, a novel design of all-optical logic gates using nonlinear directional couplers based on slot waveguides[13-15] is proposed. NOT, OR, and AND logic gates can be realized by simple single optical directional coupler configuration, and therefore, they are easy to cascade. Strong polarization dependencies of slot waveguides are effectively utilized for realizing polarization-independent optical directional couplers in linear regime and polarization-dependent all-optical switches in nonlinear regime. All the simulations performed in this paper are done for 3-D nonlinear channel waveguide structures by using rigorous numerical schemes based on full-vector finite-element method (FEM) specially formulated for nonlinear optical waveguides.[16,17] This paper is organized as follows. In section 2, we show that polarization-independent optical directional couplers can be realized by using slot waveguides.[15] In section 3, unusual nonlinear switching properties of polarization-independent slot waveguide couplers and their applications to all-optical logic gates are presented followed by conclusions in section 4.

2. Polarization-independent slot waveguide couplers

Slot waveguides were originally proposed for light confinement in the low refractive index material surrounded by high refractive index materials. In the slot waveguide, low refractive index material (slot region) is sandwiched by high refractive index materials as shown in Fig. 1. In such waveguide geometry, the guided mode polarized to one of the major axis (in this paper, *x*: quasi-TE modes) is strongly confined in the low-index slot region[13,14] because of the electric field discontinuity between high refractive index and low refractive index materials, so light can be strongly confined in the low-index slot region by total internal reflections. Since these modes are truely guided modes, there are no confinement losses. Some optical devices such as ring resonators based on slot waveguides were proposed as novel ultrasmall devices for future integrated photonics.[14,15,18-20] Of course, there exist guided modes for another major axis (*y*). These guided modes (quasi-TM modes) have very different properties compared with quasi-TE modes. By using these differences, it is possible to realize polarization-independent optical directional couplers.

Here, we consider a slot waveguide coupler as shown in Fig. 1. Waveguide parameters for the isolated slot waveguide are as follows: the refractive index of high index region and cladding are taken as n_H = 3.48 (Si) and n_C = 1.46 (SiO_2), respectively, the waveguide height h = 250 nm, and w_H = 200 nm. w_S is the width of slot region and n_S is the refractive index of slot region. The distance between two cores is d and the operating wavelength is assumed to be 1.55 μm. Fig. 2 shows the coupling length L_c of the directional coupler based on slot waveguides with w_S = 100 nm for d = 1.5 μm as a function of n_S obtained by using full-vector finite-element method (FEM).[17] We can see that the coupling length for quasi-TE modes is very sensitive to n_S while the coupling length for quasi-TM modes does not change much. This is because that for quasi-TE modes, the electric field is strongly confined in the slot region and thus, the coupling length

for quasi-TE modes is strongly influenced by the value of n_S. As a result, there is a crossing point in the L_c curves as shown in Fig. 2, at which coupling lengths for quasi-TE and TM modes are identical. The values of L_c and n_S to achieve polarization-independent operation are 203 μm and n_S = 1.41545 for d = 1.5 μm. This condition can be simply tuned by structural parameters. Fig. 3 shows the normalized output powers in the incident slot waveguide of the coupler with w_S = 100 nm, n_S = 1.41545, and d = 1.5 μm, as a function of propagation distance obtained by using finite-element beam propagation method.[16] Coupling lengths for both polarized modes are the same and the polarization-independent operation is confirmed.

3. All-optical logic gates based on nonlinear slot waveguide couplers

3-1. Unusual switching properties of nonlinear slot waveguide couplers

Here, we consider a nonlinear slot waveguide coupler as shown in Fig. 1. All the waveguide parameters and the operating wavelength are the same as in the previous section except the value of n_S. We assume that the material embedded in the slot region has Kerr-type nonlinearity, and its intensity-dependent refractive index is given by

$$n_S = n_L \sqrt{1 + \frac{n_2 \mid \boldsymbol{E} \mid^2}{Z_0}} \tag{1}$$

where n_L = 1.41545 is the linear part of the refractive index n_S, n_2 [m^2/W] is the nonlinear coefficient, $\boldsymbol{E}$ is the electric field distributions, and Z_0 is the free-space impedance. This coupler acts as a polarization-independent coupler in linear regime. Fig. 4 shows the normalized output powers in the incident slot waveguide of the coupler as a function of propagation distance for n_2P = 0.0012 μm^2. Here, P is the optical power. For quasi-TE modes, the output is switched to the incident waveguide because of phase mismatch induced by nonlinearity. However, for quasi-

TM modes, there are almost no changes in transmission characteristics compared with the linear case (black dots in Fig. 3). Fig. 5 (a) shows the normalized optical powers in the bar and cross ports of the coupler as a function of n_2P at the propagation distance of 200 μm (coupling length in linear case). Here, bar and cross ports are the outputs of the waveguides for light incidence and non-incidence, respectively. Intensity-dependent switching characteristics for quasi-TE modes can be clearly seen. Surprisingly, for quasi-TM modes, there are almost no changes in the transmission characteristics even when high intensity light is launched. This is quite unusual because in the conventional nonlinear directional coupler, switching powers for both polarizations are similar although they are polarization dependent.[4,16] This strong polarization dependence can be understood from the guided mode field distributions of quasi-TE and quasi-TM modes as shown in Figs. 5 (b) and (c), respectively. In these figures, the dominant electric fields (x and y components of electric fields, E_x and E_y, for quasi-TE and quasi-TM modes, respectively) are shown. We can see that the light is strongly confined in the slot region for quasi-TE modes while for quasi-TM modes, the fields are spreaded into the cladding region. Therefore, even if the guided mode with the same optical power is launched, a change in the propagation characteristics of quasi-TE modes caused by the nonlinearity is significantly different from that of quasi-TM modes resulting in strong polarization dependent switching characteristics. If we use Si nanocrystals[18] as a nonlinear material whose nonlinear coefficient n_2 is four orders of magnitude larger than that of SiO_2, the switching power is on the order of tens of Watt. The switching power can be further reduced by optimizing structural parameters, for example, larger separation of two cores (larger value of d) will reduce the switching power. If we increase the value of d to 1.75 μm, the value of n_S to achieve polarization-independent operation is 1.4376 for the same structural parameters. Coupling length in the linear regime for this

structure is 596 μm. Fig. 5 (d) shows the normalized output powers in the bar and cross ports of the coupler as a function of n_2P at the propagation distance of 596 μm. We can see that the switching power for quasi-TE modes is reduced to 1/3 of the previous structure. Although only one structure adopted in Fig. 5 (a) is considered in this paper, the proposed coupler with reduced switching power or structural parameters for easier fabrication can be designed using different materials and different structural parameters in a similar way.

3-2. NOT gate

Here, we consider an all-optical NOT gate based on nonlinear slot waveguide couplers. The schematic of the structure is shown in Fig. 6. In this device, there are one input port A and two output ports C and D. A quasi-TM mode with the optical power P is launched from port A as a signal light whose logical input state is denoted by Y_i. The signal light is coupled to another waveguide (port D) at the coupling length if no perturbations induced by nonlinearity are added as shown in Fig. 7 (a). When a quasi-TE mode with the same optical power P which is above the switching power is simultaneously launched from port A as a control light whose logical input state is denoted by X_i, the control light is not coupled to another waveguide and the optical power of control light remains in the incident waveguide (port C) at the coupling length (see Fig. 5(a)). If the optical power P is high enough to add perturbations induced by nonlinearity for the signal light, the signal light will not coupled to port D because of phase mismatch and the output will be inverted as shown in Fig. 7 (b). These input and output characteristics are summarized in Table 1 in which logical output state in port D is denoted by X_o. Logical state of X_o is reversed compared with logical state of X_i showing the inverting operation, namely, when the control light (quasi-TE mode) is not launched, the signal light is coupled to port D, on the other hand, when

the control light is launched, the signal light is not coupled to port D resulting in no outputs to port D. Fig. 8 shows the normalized signal light powers in ports C and D, where the control light is simultaneously launched to port A and the distance between input and output ports is 200 μm (coupling length in linear regime). The transmission characteristics of the signal light with simultaneous control light incidence are calculated as follows. First, beam propagation simulation is performed for the control light (quasi-TE mode) incidence. Next, beam propagation simulation for the signal light (quasi-TM mode) is carried out using the field distributions of the control light for calculating nonlinear refractive index distributions. This method is valid when the instantaneous Kerr-type nonlinearity is considered. We can see that the output to port D is switched to port C by increasing n_2P. It means that by launching the control light, the output to port D is inverted resulting in NOT gate operation. The switching power is increased compared with the self-switching power of quasi-TE modes shown in Fig. 5 (a). This is due to the fact that the quasi-TM mode is less sensitive to the refractive index change in the slot region. Figs. 9 show the field distributions of quasi-TM mode without quasi-TE mode incidence at the propagation distance of (a) 0, (b) 100, and (c) 200 μm, respectively, for n_2P = 0.005 μm^2 (corresponds to X_i = 0). The incident field is coupled to another port and the output to port D is "1" at 200 μm (X_o = 1). Figs. 10 (a), (b), and (c) show the field distributions of quasi-TM mode with quasi-TE mode incidence at the propagation distance of 0, 100, and 200 μm, respectively, for n_2P = 0.005 μm^2 (corresponds to X_i = 1). We can see that the launched field is not completely coupled to port D and the output to port D is "0" at 200 μm (X_o = 0).

3-3. OR and AND gates

Here, we consider all-optical OR and AND gates based on nonlinear slot waveguide couplers as shown in Fig. 11. In this device, there are two input ports A and B, and two output ports C and D. The quasi-TE mode of the waveguide with the optical power P is launched to port A as one of the logical input and the quasi-TM mode with the same optical power is launched to port B as another logical input. The schematics of logical operations are shown in Fig. 12 and in the following discussion, notations (X_i, Y_i) and (X_o, Y_o) are used for logical input and output of the device, respectively. Here, X_i and Y_i are 0 or 1 corresponding to logical input to ports A and B, respectively. X_o and Y_o are 0 or 1 corresponding to logical output to ports C and D. For (X_i, Y_i) = (1, 0) input (only the quasi-TE mode is launched to port A), incident quasi-TE mode is not coupled to another waveguide if the optical power P is above the switching power and the output to port C is "1" as shown in Fig. 12 (a), namely, (X_o, Y_o) = (1, 0). For (X_i, Y_i) = (0, 1) input (only the quasi-TM mode is launched to port A), incident quasi-TM mode is coupled to another waveguide because of unusual properties of nonlinear slot waveguide couplers as described in 3-1 and the output to port C is "1" as shown in Fig. 12 (b), namely, (X_o, Y_o) = (1, 0). For (X_i, Y_i) = (1, 1) input (quasi-TE and quasi-TM modes are launched to ports A and B, respectively), incident quasi-TE mode remains in port C if the optical power P is above the switching power. The output of quasi-TM mode depends on the optical power P. If the optical power P is high enough to induce phase mismatch, the quasi-TM mode is not coupled to another waveguide as shown in Fig. 12 (c), namely, (X_o, Y_o) = (1, 1). These input and output characteristics are summarized in Table 2. As is evident from Table 2, ports C and D act as OR and AND gates, respectively. Fig. 13 shows the normalized powers of quasi-TM modes in ports C and D as a function of n_2P, where the distance between input and output ports is 200 μm. The output is switched to port D for larger values of n_2P as expected. Figs. 14 (a), (b), and (c) show the field

distributions at the propagation distance of 0, 100, and 200 μm, respectively, for (X_i, Y_i) = (1, 0) input and n_2P = 0.006 μm^2. The incident mode is not coupled to another waveguide, resulting in (X_o, Y_o) = (1, 0) output. Figs. 15 (a), (b), and (c) show the field distributions at the propagation distance of 0, 100, and 200 μm, respectively, for (X_i, Y_i) = (0, 1) input and n_2P = 0.006 μm^2. The incident mode is coupled to another waveguide resulting in (X_o, Y_o) = (1, 0) output. Figs. 16 (a), (b), and (c) show the field distributions at the propagation distance of 0, 100, and 200 μm, respectively, for (X_i, Y_i) = (1, 1) input and n_2P = 0.006 μm^2. Here, only the field distributions of quasi-TM mode are shown. Both modes are not coupled to their cross ports resulting in (X_o, Y_o) = (1, 1) output. It should be noted that although these logic gates are easy to cascade because of their simple configuration, in some cases, waveguide type polarization controllers[21,22], mode shape converters and amplifiers would be required to connect two logic gates. This can be a great advantage compared with logic gates proposed in the past.

4. Conclusion

We have proposed a novel design of all-optical logic gates based on nonlinear slot waveguide couplers. The proposed slot waveguide coupler acts as a polarization-independent coupler in linear regime and shows the strong polarization-dependent switching characteristics in nonlinear regime. By using these unusual characteristics effectively, NOT, OR, and AND logic gates can be realized with a single directional coupler. Proposed logic gates are easy to cascade because of their structural simplicity and the full 3-D optical waveguide structure is considered.

T. Fujisawa's e-mail address is fujisawa@dpo7.ice.eng.hokudai.ac.jp

References

1. G.I. Stegeman, E.M. Wright, N. Filayson, R. Zanoni, and C.T. Seaton, “Third order nonlinear integrated optics,” J. Lightwave Technol., **6**, 953-970 (1988).
2. S.M. Jensen, “The nonlinear coherent coupler,” IEEE J. Quantum Electron., **QE-18**, 1580–1583 (1982).
3. F. Di Pasquale and H.E. Hernandez-Figueroa, “Improved all-optical switching in a three-slab nonlinear directional coupler with gain,” IEEE J. Quantum Electron., **30**, 1254-1258 (1994).
4. S.S.A. Obayya, B.M.A. Rahman, and H.A. El-Mikati, “Full-vectorial finite-element beam propagation method for nonlinear directional coupler devices,” IEEE J. Quantum Electron., **36**, 556-562 (2000).
5. J.S. Aitchison, A.H. Kean, C.N. Ironside, A. Villeneuve, and G.I. Stegeman, “Ultrafast all-optical switching in $Al_{0.18}Ga_{0.82}As$ directional coupler in 1.55 μm spectral region,” Electron. Lett., **27**, 1709-1710 (1991).
6. J.-M. Jeong and M.E. Marhic, “All-optical logic gates based on cross-phase modulation in a nonlinear fiber interferometer,” Opt. Commun., **85**, 430-436 (1991).
7. G. Cancellieri, F. Chiaraluce, E. Gambi, and P. Pierleoni, “Coupled-soliton photonic logic gates: practical design procedures,” J. Opt. Soc. Am. B, **12**, 1300-1306 (1995).
8. A. Niiyama and M. Koshiba, “Three-dimensional beam propagation analysis of nonlinear optical fibers and optical logic gates,” J. Lightwave Technol., **16**, 162-168 (1998).
9. Y. Wang and J. Liu, “All-fiber logical devices based on the nonlinear directional coupler,” IEEE Photon. Technol. Lett., **11**, 72-74 (1999).

10. M. Zitelli, E. Fazio, and M. Bertolotti, “All-optical NOR gate based on the interaction between cosine-shaped input beams of orthogonal polarization,” J. Opt. Soc. Am. B, **16**, 214-218 (1999).
11. T. Yabu, M. Geshiro, T. Kitamura, K. Nishida, and S. Sawa, “All-optical logic gates containing a two-mode nonlinear waveguides,” IEEE J. Quantum Electron., **38**, 37-46 (2002).
12. Y.-D. Wu, “All-optical logic gates by using multibranch waveguide structure with localized optical nonlinearity,” IEEE J. Sel. Topics Quantum Electron., **11**, 307-312 (2005).
13. V.R. Almeida, Q. Xu, C.A. Barrios, and M. Lipson, “Guiding and confining light in void nanostructures,” Opt. Lett, **29**, 1209-1211 (2004).
14. Q. Xu, V.R. Almeida, R.R. Panepucci, and M. Lipson, “Experimental demonstration of guiding and confining light in nanometer-size low-refractive-indx material,” Opt. Lett., **29**, 1626-1628 (2004).
15. T. Fujisawa and M. Koshiba, “A polarization independent optical directional coupler based on slot waveguides,” Opt. Lett., accepted for publication.
16. T. Fujisawa and M. Koshiba, “Full-vector finite-element beam propagation method for three-dimensional nonlinear optical waveguides,” J. Lightwave Technol., **20**, 1876-1884 (2002).
17. T. Fujisawa and M. Koshiba, “Finite element characterization of chromatic dispersion in nonlinear holey fibers,” Opt. Express, **11**, 1481-1489 (2003).
18. C.A. Barrios, “High-performance all-optical silicon microswitch,” Electron. Lett., **40**, 862-863 (2004).

19. T.B. Jones, M. Hochberg, C. Walker, and A. Scherer, “High-Q optical resonators in silicon-on-insulator-based slot waveguides,” Appl. Phys. Lett., **86**, 081101 (2005).
20. T.B. Jones, M. Hochberg, G. Wang, R. Lawson, Y. Liao, P.A. Sullivan, L. Dalton, A.K.-Y. Jen, and A. Scherer, “Optical modulation and detection in slotted silicon waveguides,” Opt. Express, **13**, 5216-5226 (2005).
21. M.R. Watts and H.A. Haus, “Integrated mode-evolution-based polarization rotators,” Opt. Lett., **30**, 138-140 (2005).
22. H. Deng, D.O. Yevick, C. Brooks, and P.E. Jessop, “Design rules for slanted-angle polarization rotators,” J. Lightwave Technol., **23**, 432-445 (2005).

List of Table Captions

Table 1. Logical input and output characteristics of the structure shown in Fig. 6. Port D acts as NOT gate for the input of quasi-TE mode.

Table 2. Logical input and output characteristics of the structure shown in Fig. 11. Ports C and D act as OR and AND gates, respectively.

List of Figure Captions

Fig. 1. A slot waveguide coupler.

Fig. 2. Coupling lengths of the slot waveguide coupler as a function of n_s for d = 1.5 μm.

Fig. 3 Normalized optical power in the incident slot waveguide of the coupler with w_S = 100 nm, n_S = 1.41545, and d = 1.5 μm as a function of propagation distance.

Fig. 4 Normalized output powers in the incident slot waveguide of the coupler as a function of propagation distance for n_2P = 0.0012 μm^2.

Fig. 5 (a) Normalized optical powers in the bar and cross ports of the coupler as a function of n_2P at the propagation distance of 200 μm. Field distributions of linear guided (b) quasi-TE and (c) quasi-TM modes of the slot waveguide. (d) Normalized optical powers in the bar and cross ports of the coupler as a function of n_2P at the propagation distance of 596 μm with d = 1.75 μm.

Fig. 6 NOT gate based on nonlinear slot waveguide couplers.

Fig. 7 NOT gate operation. (a) $X_i = 0$ input and (b) $X_i = 1$ input.

Fig. 8 Normalized signal light powers in ports C and D, where the control light is simultaneously launched to port A and the distance between input and output ports is 200 μm.

Fig. 9 Field distributions of quasi-TM mode without quasi-TE mode incidence at the propagation distance of (a) 0, (b) 100, and (c) 200 μm, respectively, for $n_2P = 0.005$ μm^2.

Fig. 10 Field distributions of quasi-TM mode with quasi-TE mode incidence at the propagation distance of (a) 0, (b) 100, and (c) 200 μm, respectively, for $n_2P = 0.005$ μm^2.

Fig. 11 All-optical OR and AND gates based on nonlinear slot waveguide couplers.

Fig. 12 OR and AND gates operations. (a) $(X_i, Y_i) = (1, 0)$ input, (b) $(X_i, Y_i) = (0, 1)$ input, and (c) $(X_i, Y_i) = (1, 1)$ input.

Fig. 13 Normalized powers of quasi-TM modes in ports C and D as a function of n_2P, where the distance between input and output ports is 200 μm.

Fig. 14 Field distributions at the propagation distance of (a) 0, (b) 100, and (c) 200 μm, respectively, for $(X_i, Y_i) = (1, 0)$ input and $n_2P = 0.006$ μm^2.

Fig. 15 Field distributions at the propagation distance of (a) 0, (b) 100, and (c) 200 μm, respectively, for $(X_i, Y_i) = (0, 1)$ input and $n_2P = 0.006$ μm^2.

Fig. 16 Field distributions at the propagation distance of (a) 0, (b) 100, and (c) 200 μm, respectively, for $(X_i, Y_i) = (1, 1)$ input and $n_2P = 0.006$ μm^2. Only the field distributions of quasi-TM modes are shown.

Table 1. Logical input and output characteristics of the structure shown in Fig. 6.

Port D acts as NOT gate for the input of quasi-TE mode.

X_i	Y_i	X_o
0	**1**	**1**
1	**1**	**0**

Table 2. Logical input and output characteristics of the structure shown in Fig. 11.

Ports C and D act as OR and AND gates, respectively.

X_i	Y_i	X_o	Y_o
0	**0**	**0**	**0**
0	**1**	**1**	**0**
1	**0**	**1**	**0**
1	**1**	**1**	**1**

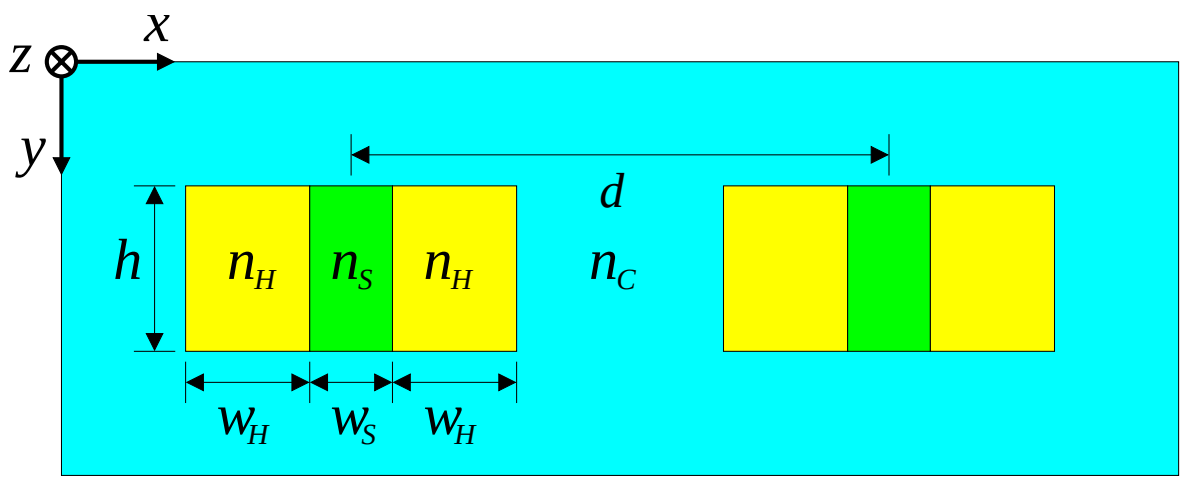

Fig. 1. A slot waveguide coupler.

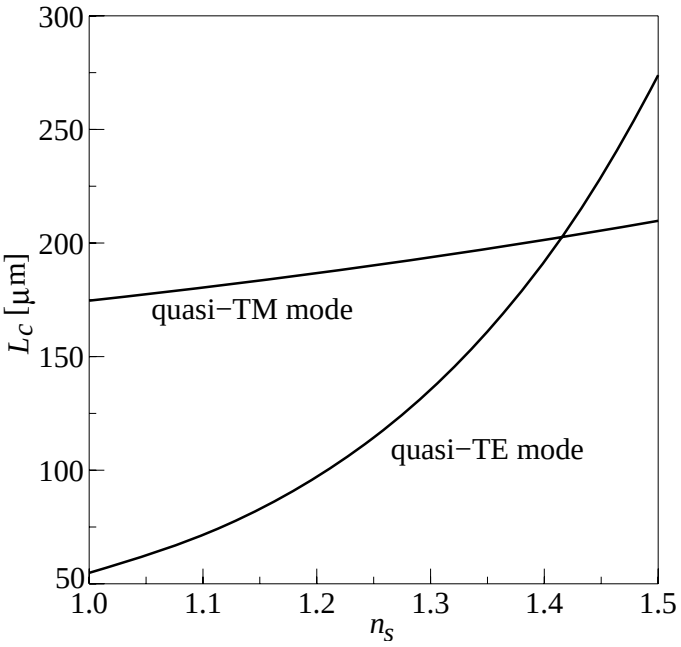

Fig. 2 Coupling lengths of the slot waveguide coupler as a function of n_s for d = 1.5 μm.

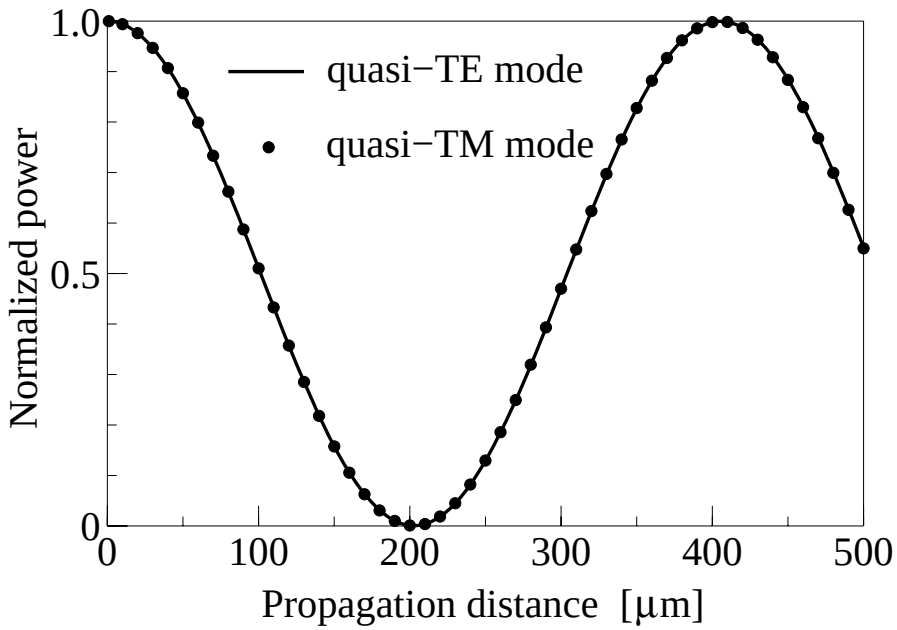

Fig. 3 Normalized optical power in the incident slot waveguide of the coupler with w_S = 100 nm, n_S = 1.41545, and d = 1.5 μm as a function of propagation distance.

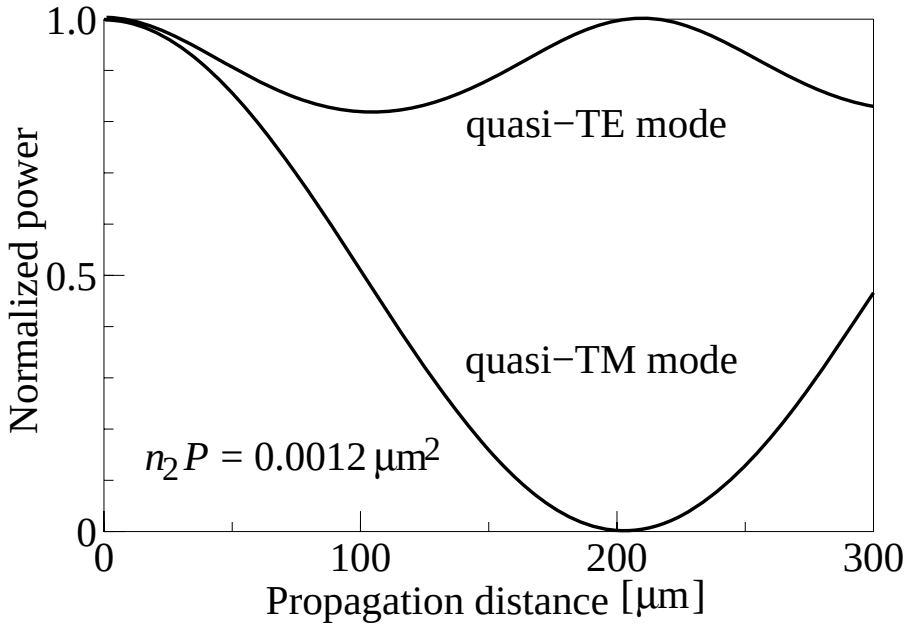

Fig. 4 Normalized output powers in the incident slot waveguide of the coupler as a function of propagation distance for $n_2P = 0.0012\ \mu m^2$.

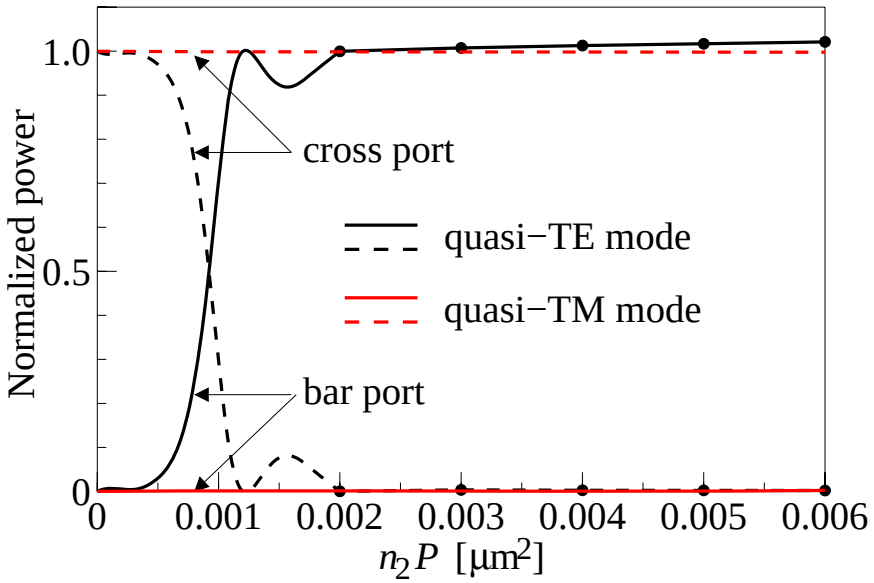
1.0
0.5
0
Normalized power
cross port
quasi−TE mode
quasi−TM mode
bar port
0
0.001
0.002
0.003
0.004
0.005
0.006
$n_2 P$ [μm^2]

(a)

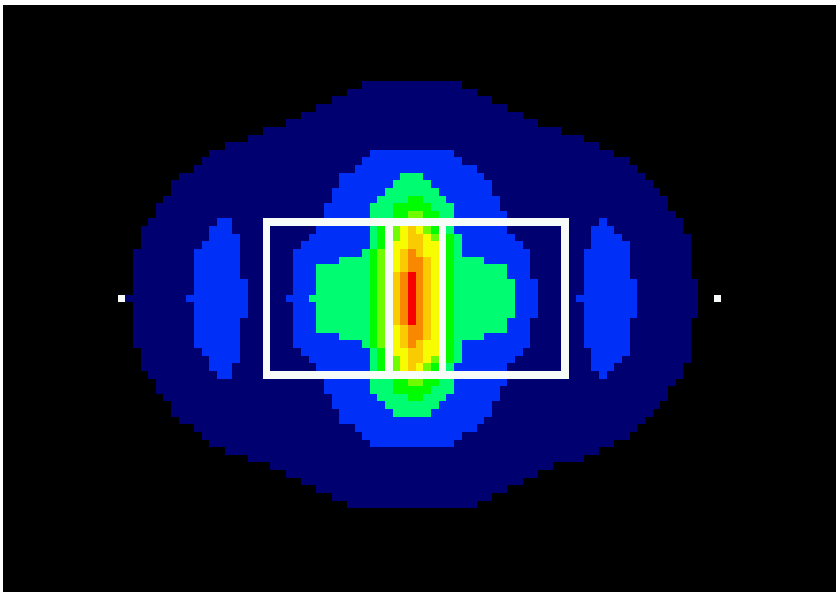

(b)

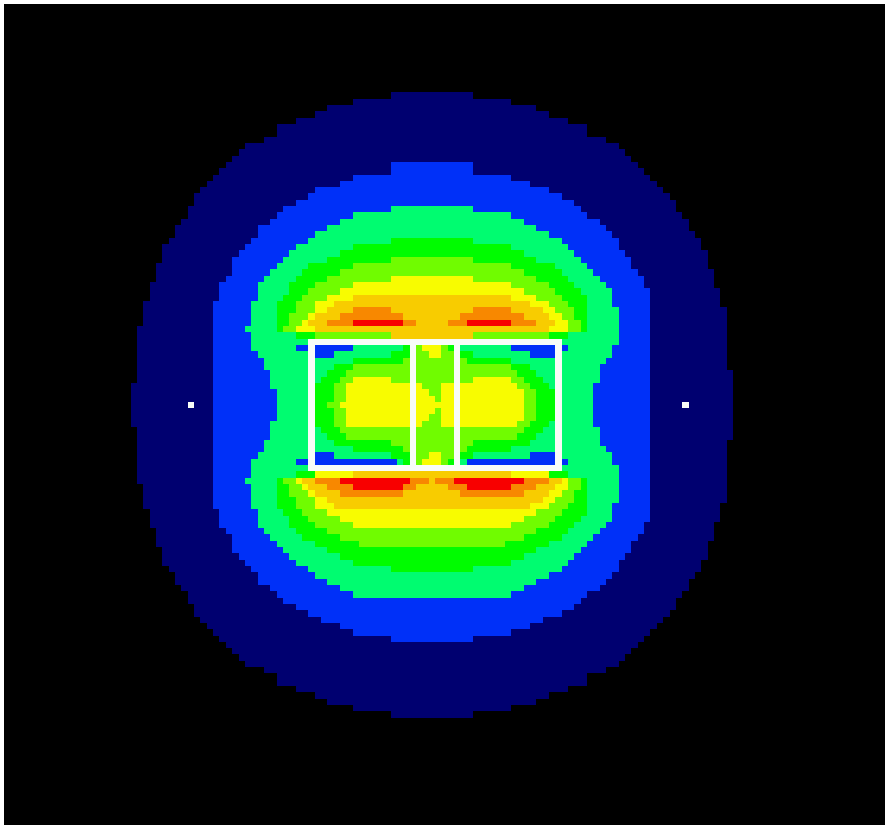

(c)

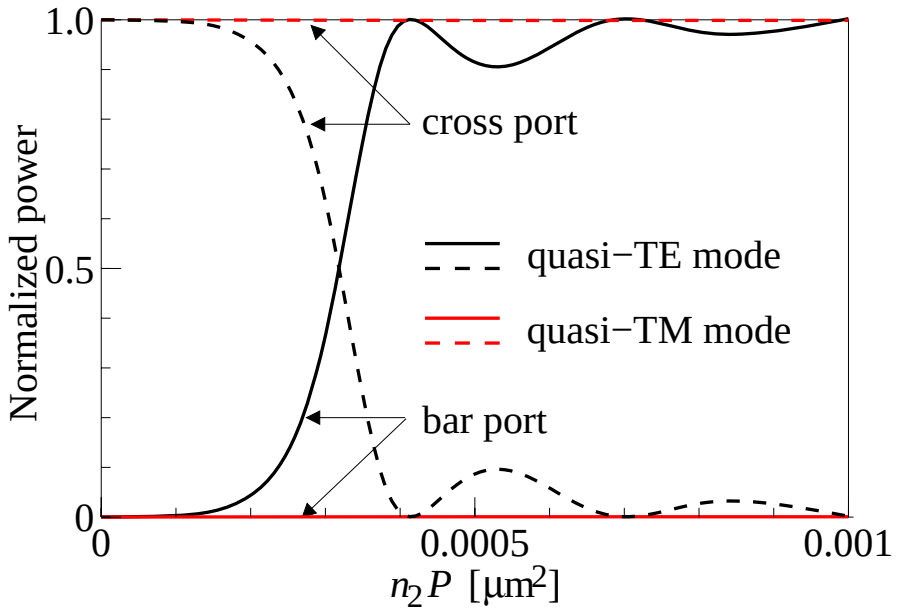

(d)

Fig. 5 (a) Normalized optical powers in the bar and cross ports of the coupler as a function of n_2P at the propagation distance of 200 μm. Field distributions of linear guided (b) quasi-TE and (c) quasi-TM modes of the slot waveguide. (d) Normalized optical powers in the bar and cross ports of the coupler as a function of n_2P at the propagation distance of 596 μm with d = 1.75 μm.

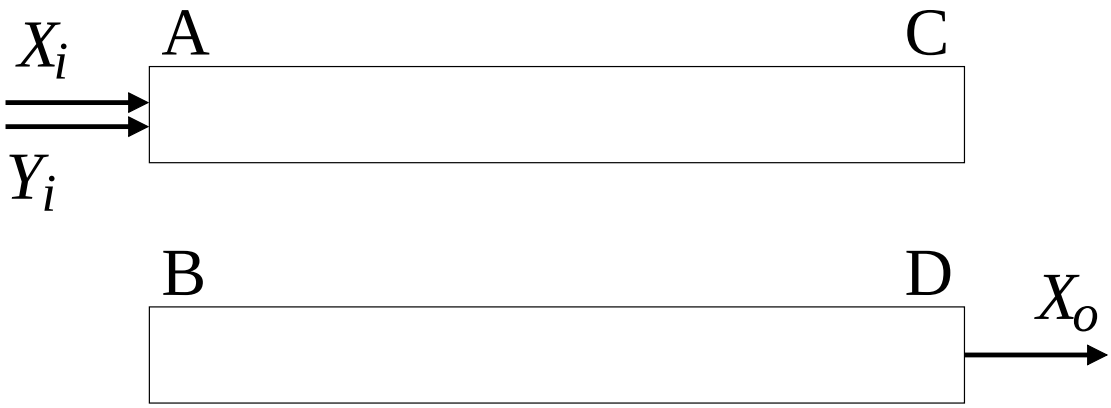

Fig. 6 NOT gate based on nonlinear slot waveguide couplers.

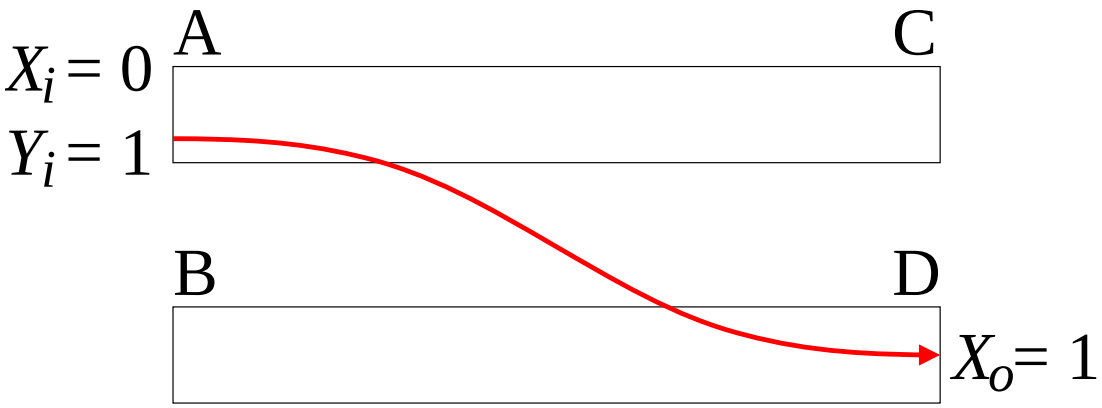

(a)

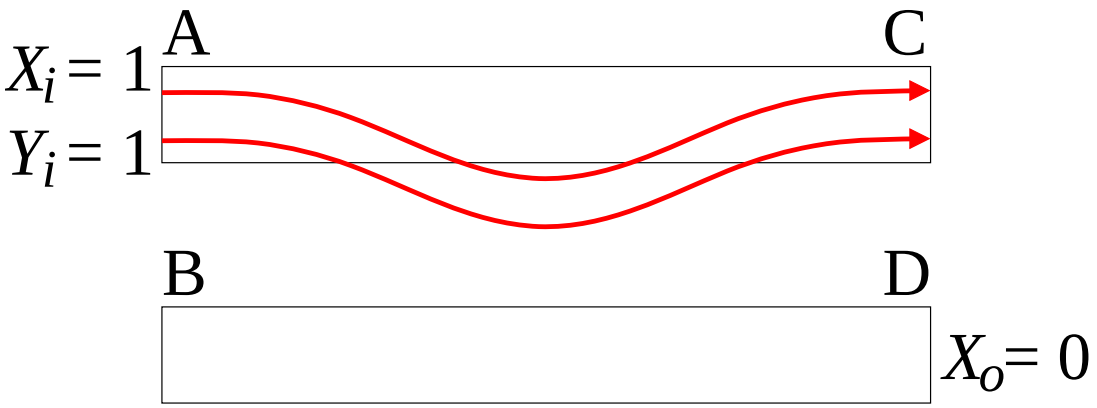

(b)

Fig. 7 NOT gate operation. (a) $X_i = 0$ input and (b) $X_i = 1$ input.

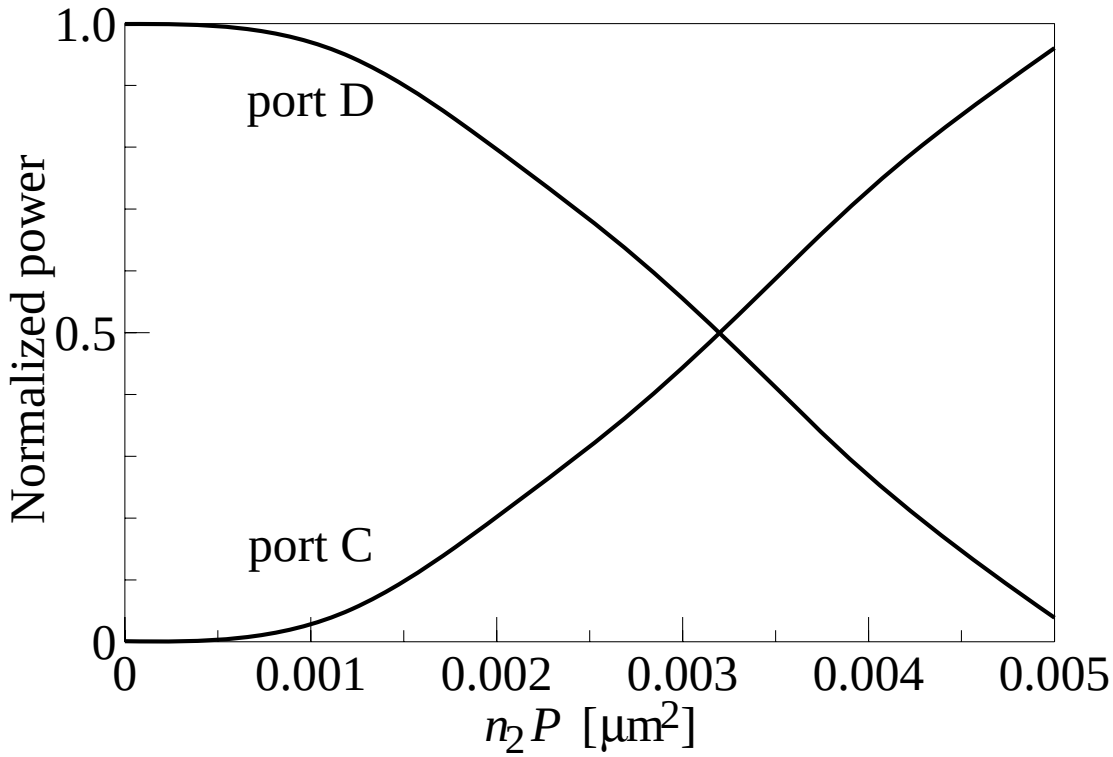

Fig. 8 Normalized signal light powers in ports C and D, where the control light is simultaneously launched to port A and the distance between input and output ports is 200 μm.

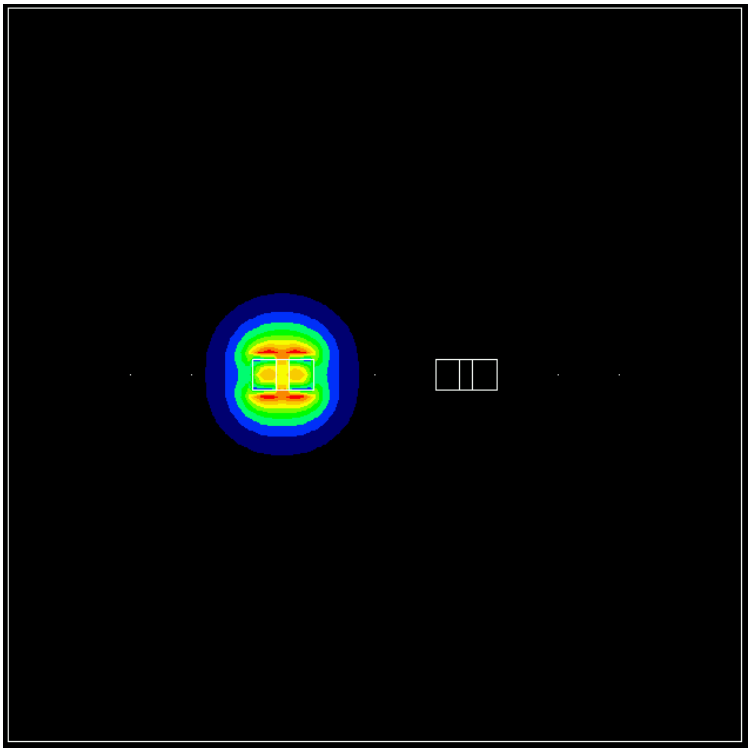

(a)

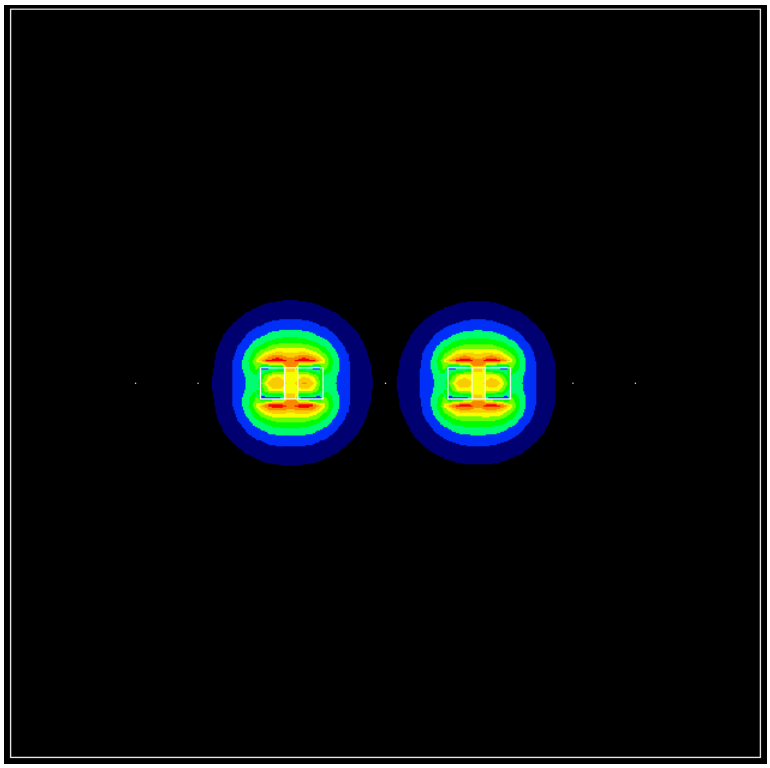

(b)

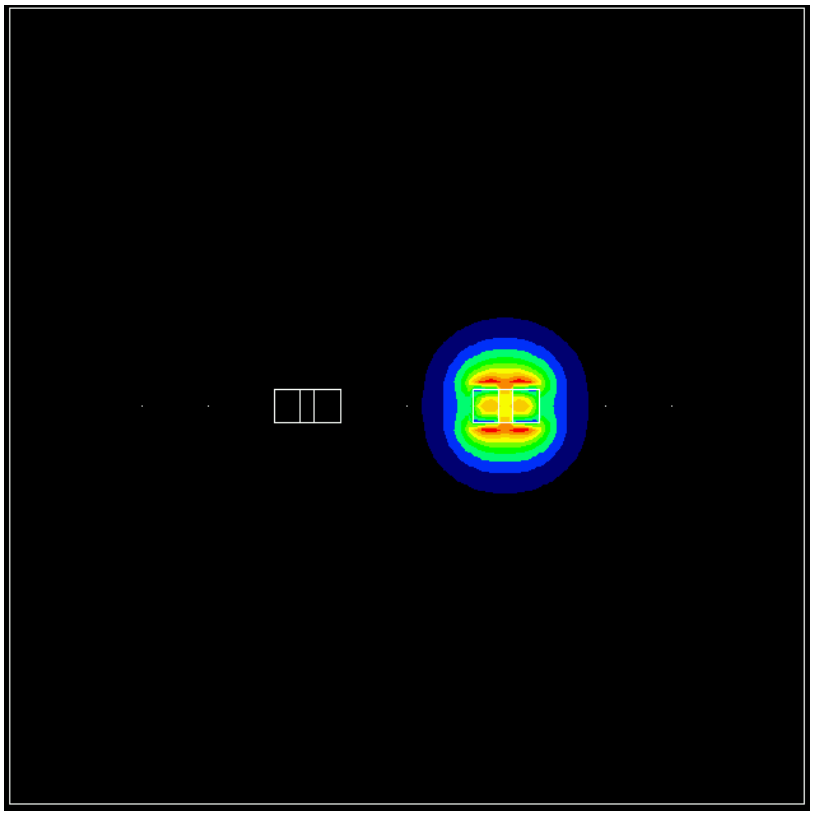

(c)

Fig. 9 Field distributions of quasi-TM mode without quasi-TE mode incidence at the propagation distance of (a) 0, (b) 100, and (c) 200 μm, respectively, for n_2P = 0.005 μm^2.

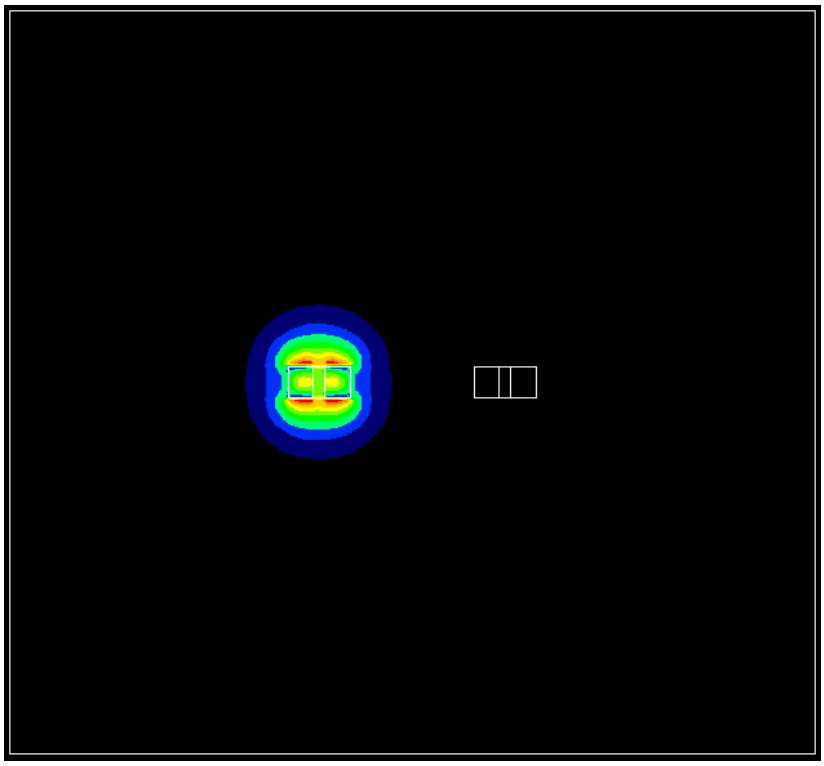

(a)

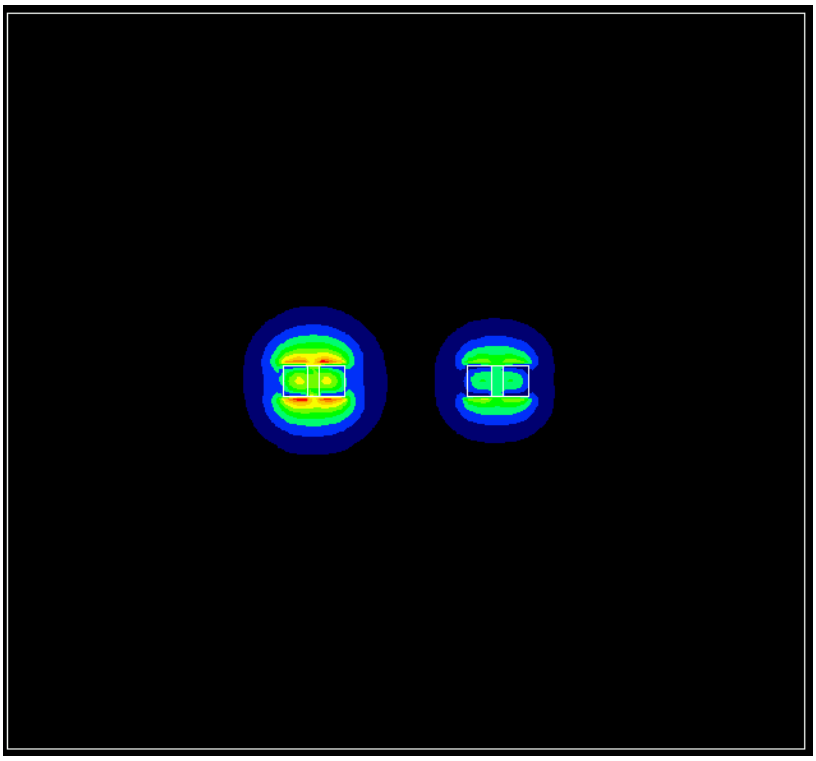

(b)

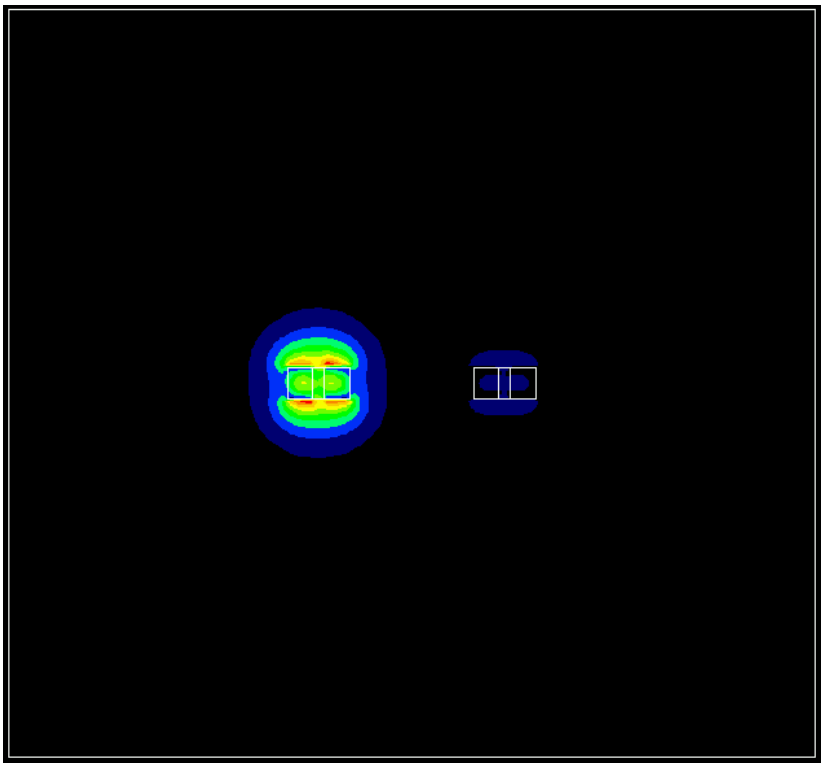

(c)

Fig. 10 Field distributions of quasi-TM mode with quasi-TE mode incidence at the propagation distance of (a) 0, (b) 100, and (c) 200 μm, respectively, for n_2P = 0.005 μm^2.

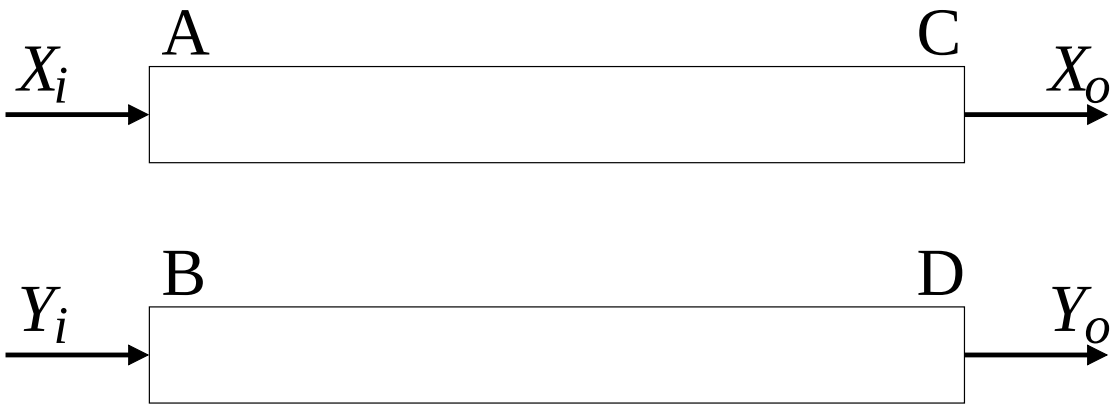

Fig. 11 All-optical OR and AND gates based on nonlinear slot waveguide couplers.

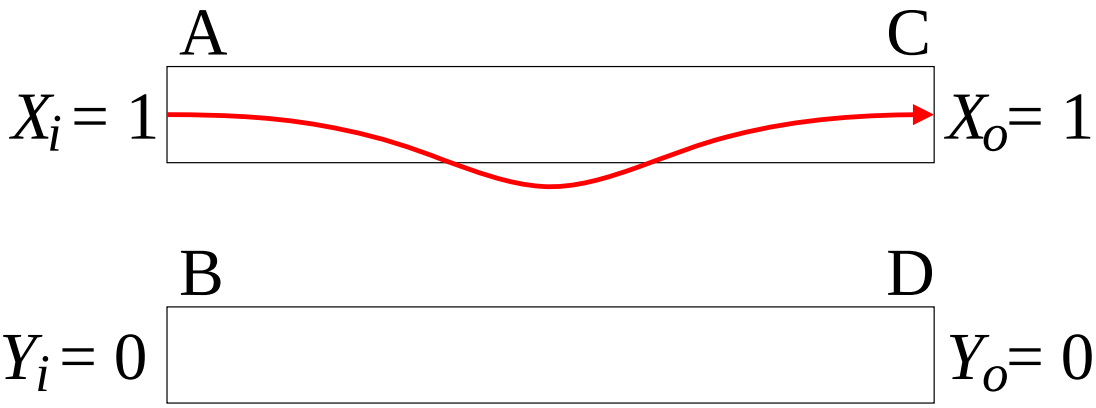

(a)

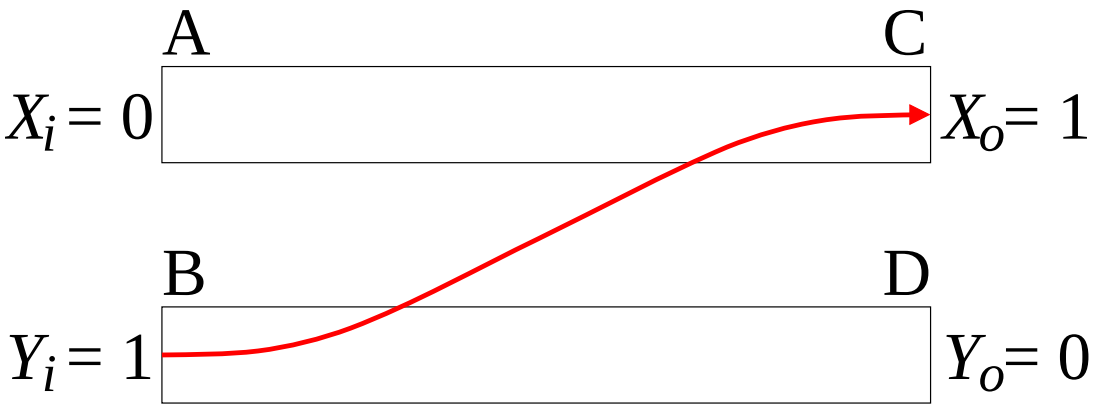

(b)

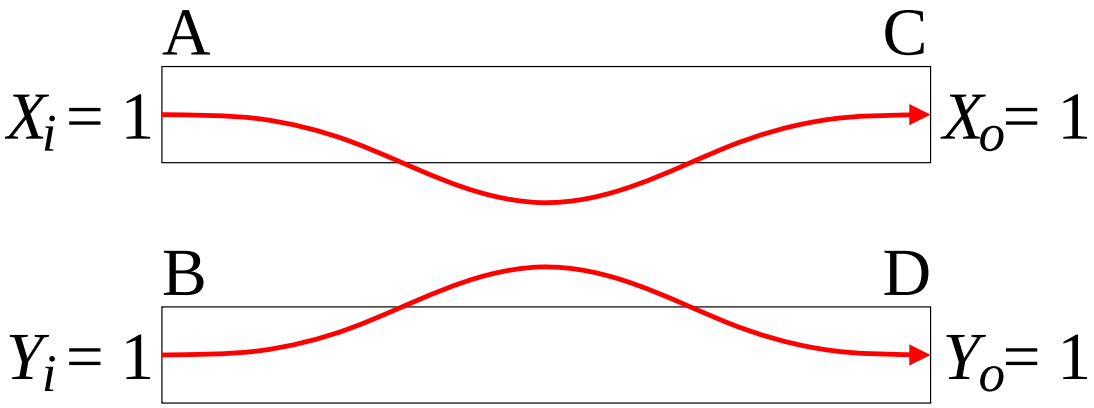

(c)

Fig. 12 OR and AND gates operations. (a) (X_i, Y_i) = (1, 0) input, (b) (X_i, Y_i) = (0, 1) input, and (c) (X_i, Y_i) = (1, 1) input.

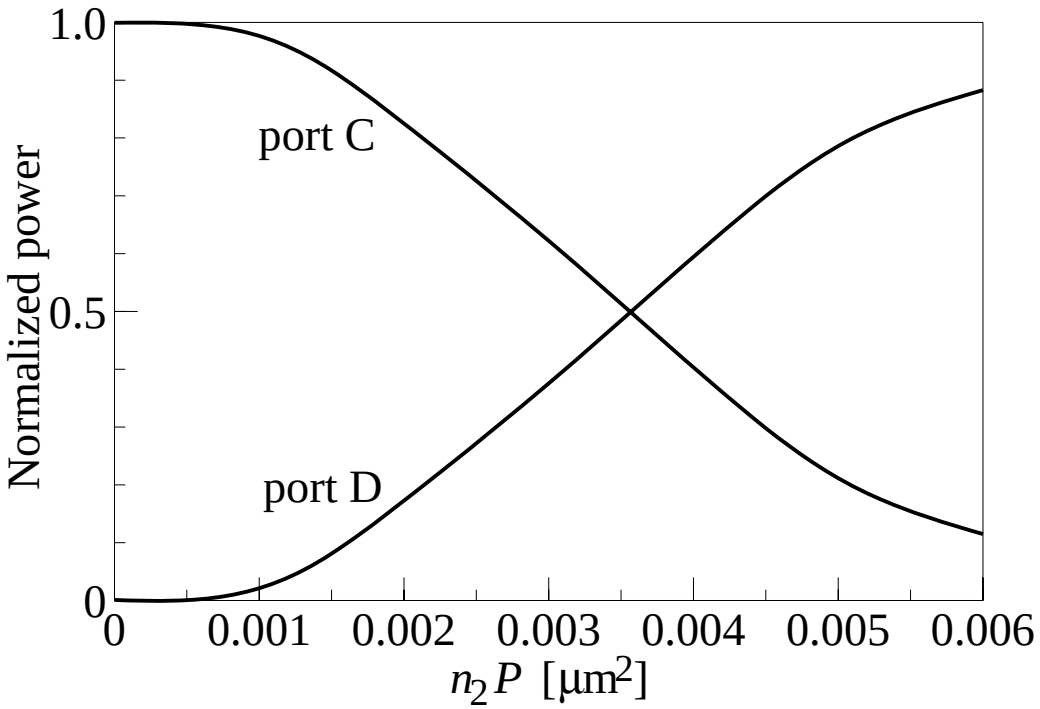

Fig. 13 Normalized powers of quasi-TM modes in ports C and D as a function of n_2P, where the distance between input and output ports is 200 μm.

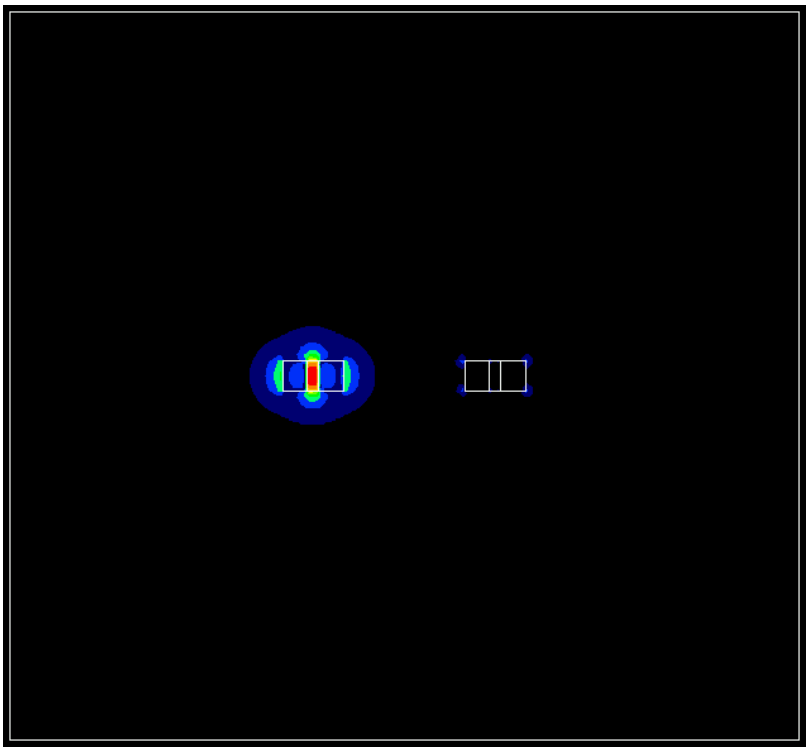

(a)

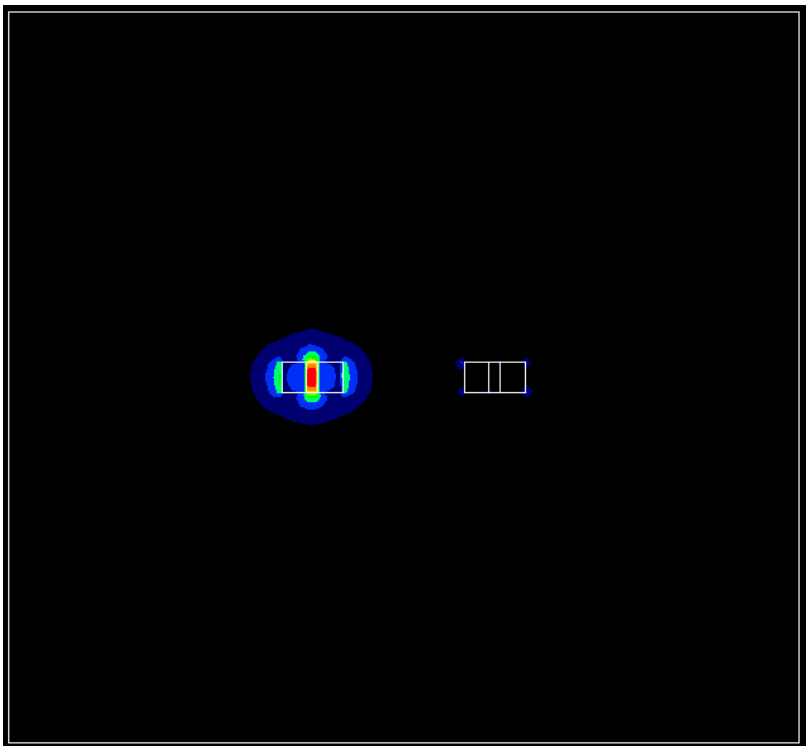

(b)

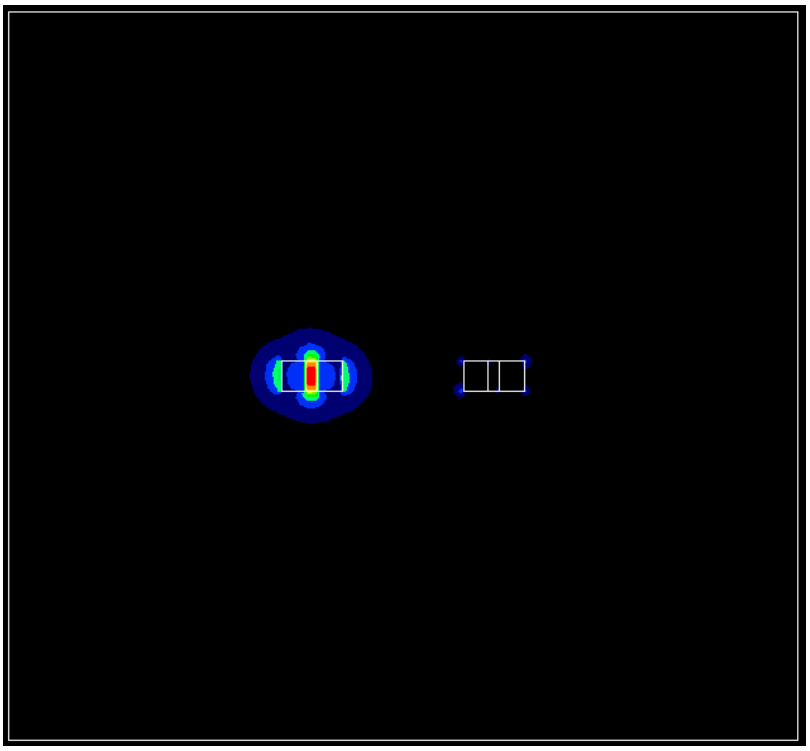

(c)

Fig. 14 Field distributions at the propagation distance of (a) 0, (b) 100, and (c) 200 μm, respectively, for $(X_i, Y_i) = (1, 0)$ input and $n_2P = 0.006$ μm^2.

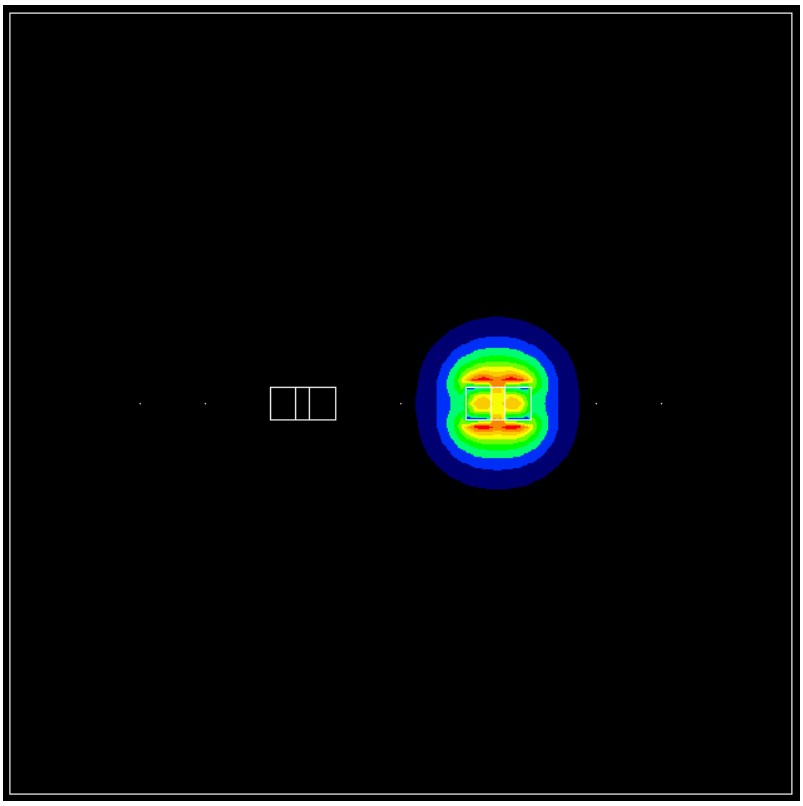

(a)

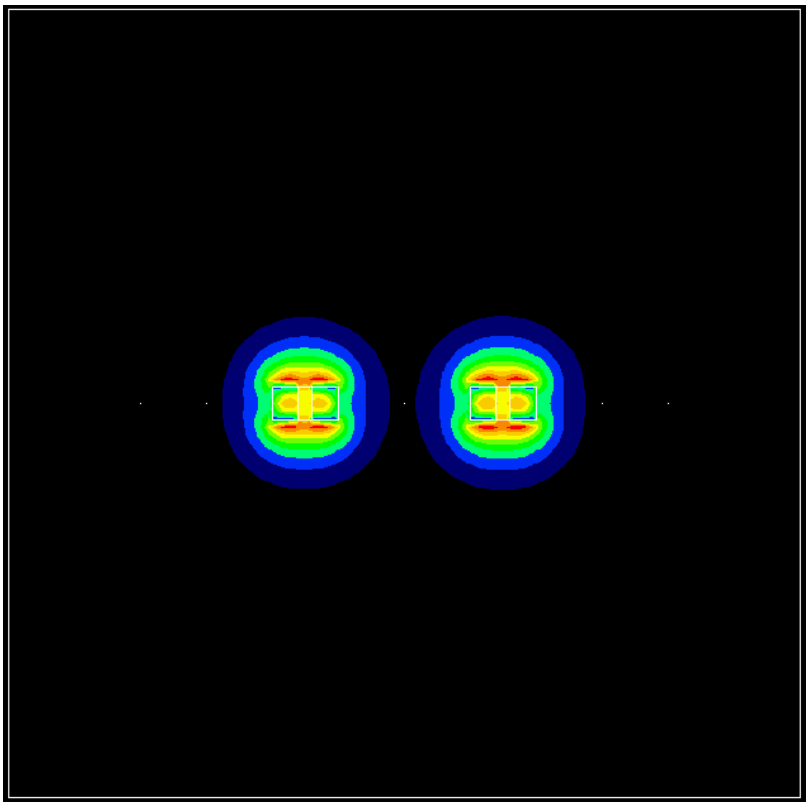

(b)

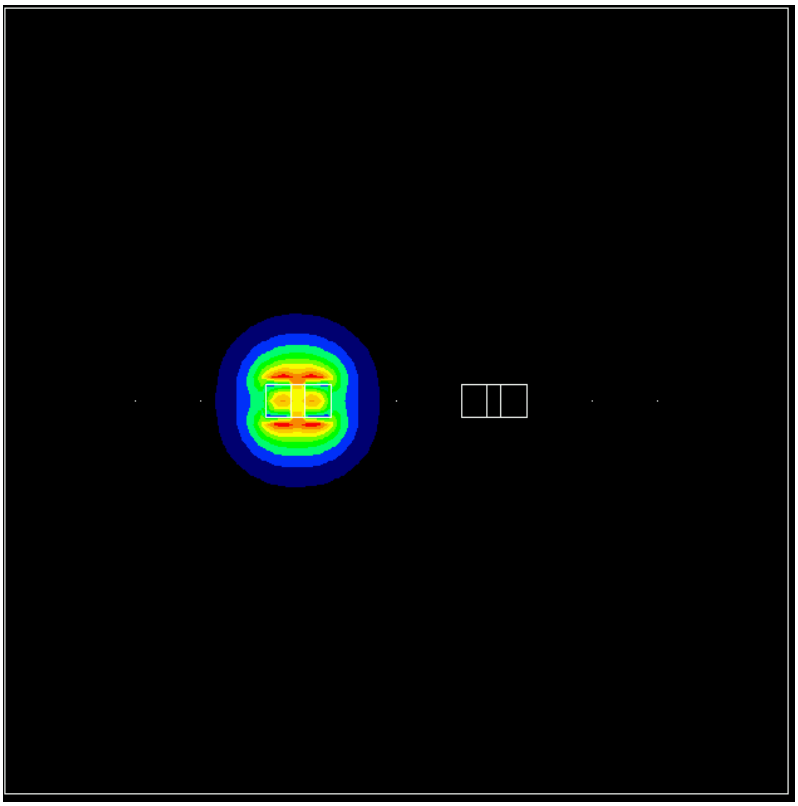

(c)

Fig. 15 Field distributions at the propagation distance of (a) 0, (b) 100, and (c) 200 μm, respectively, for $(X_i, Y_i) = (0, 1)$ input and $n_2P = 0.006$ μm^2.

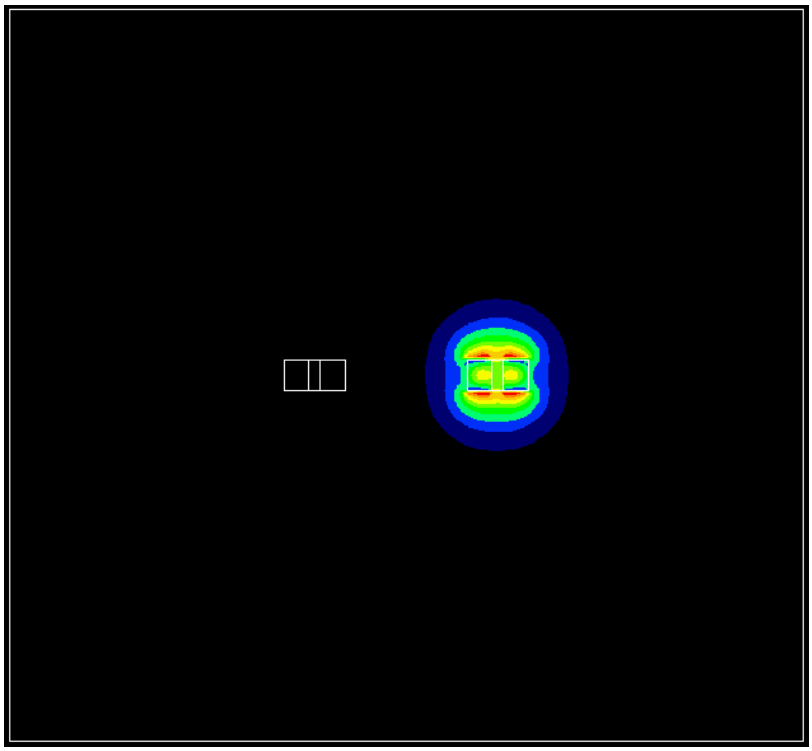

(a)

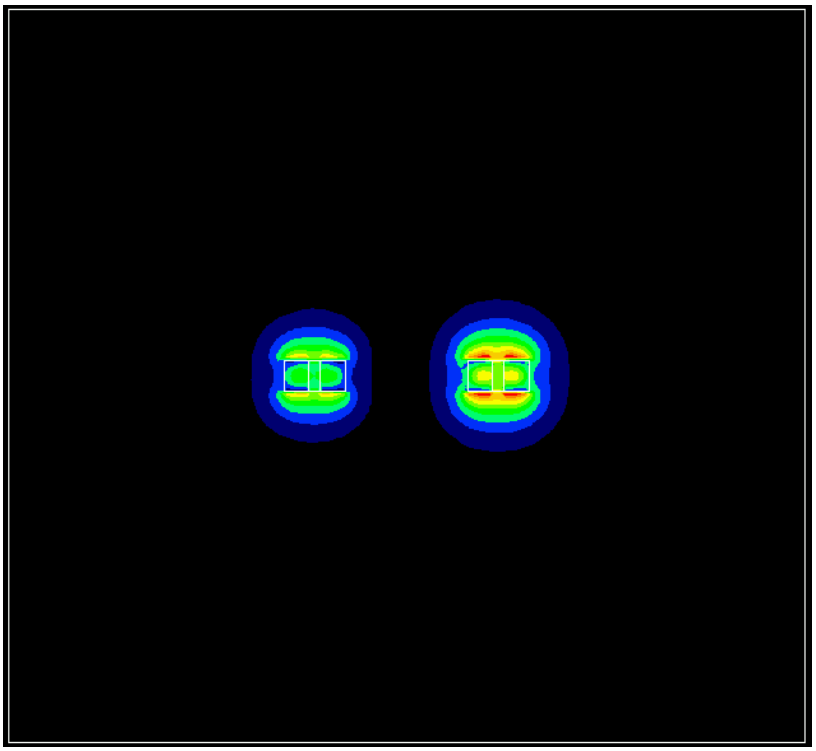

(b)

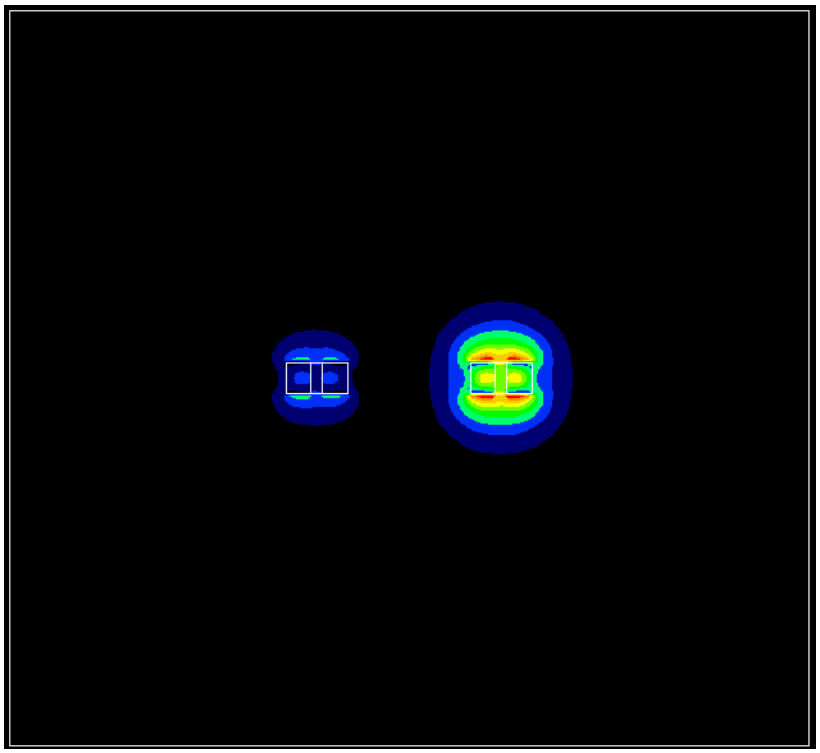

(c)

Fig. 16 Field distributions at the propagation distance of (a) 0, (b) 100, and (c) 200 μm, respectively, for (X_i, Y_i) = (1, 1) input and n_2P = 0.006 μm^2. Only the field distributions of quasi-TM modes are shown.